International Journal of Machining and Machinability of Materials

ISSN online: 1748-572X - ISSN print: 1748-5711
https://www.inderscience.com/ijmmm

Comparative machinability study of ADI-4h and mild steel using WEDM

Pranjal Sarma, Dibya Jyoti Borah, Promod Kumar Patowari, Ajay Likhite

DOI: 10.1504/IJMMM.2023.10053978

Article History:

Received:	27 September 2022
Last revised:	20 November 2022
Accepted:	01 January 2023
Published online:	15 March 2023

Comparative machinability study of ADI-4h and mild steel using WEDM

Pranjal Sarma*

Department of Mechanical Engineering,
Assam Don Bosco University,
Guwahati, 781017, Assam, India
and
Department of Mechanical Engineering,
National Institute of Technology Silchar,
Silchar, Assam, India
Email: t20pranjal@gmail.com
*Corresponding author

Dibya Jyoti Borah

Department of Mechanical Engineering,
National Institute of Technology Silchar,
Silchar, Assam, India
and
Kameng Hydro Electric Project,
NEEPCO Ltd.,
West Kameng, Arunachal Pradesh, India
Email: dibyajyotiborah49@yahoo.com

Promod Kumar Patowari

Department of Mechanical Engineering,
National Institute of Technology Silchar,
Silchar, Assam, India
Email: ppatowari@yahoo.com

Ajay Likhite

Department of Metallurgical & Materials Engineering,
Visvesvaraya National Institute of Technology,
Nagpur, Maharashtra, India
Email: aalikhite@mme.vnit.ac.in

Abstract: Austempered ductile iron (ADI) has been gaining increasing popularity due to its interesting mechanical properties. But its machining by conventional methods is difficult. We report the machining processing response of ADI-4h while processing under wire electric discharge machining (WEDM). The effect of the major WEDM process parameters viz. peak current, pulse-on-time and wire feed on the major response parameters viz. cutting rate, kerf width and surface roughness has been investigated. A comparative

machinability study is also carried out with mild steel. Study reveals that ADI shows fairly good machinability under WEDM even though mild steel is more easily machinable. SEM analysis reveals presence of nodular graphite and ausferritic microstructure on the matrix of synthesised ADI-4h and an average recast layer thickness of ~ 6 μm after WEDM processing. The study can help researcher and industries to better understand ADI machinability via WEDM and hence augment its application in various fields.

Keywords: austempered ductile iron; ADI; mild steel; wire electric discharge machining; WEDM; recast layer; machinability; microstructure; austempering.

Reference to this paper should be made as follows: Sarma, P., Borah, D.J., Patowari, P.K. and Likhite, A. (2023) 'Comparative machinability study of ADI-4h and mild steel using WEDM', *Int. J. Machining and Machinability of Materials*, Vol. 25, No. 1, pp.69–88.

Biographical notes: Pranjal Sarma is currently working as a Senior Assistant Professor, Mechanical Engineering Department, Assam Don Bosco University. He received his BE in Mechanical Engineering from Gauhati University; MTech in Design and Manufacturing from NIT Silchar and pursuing his PhD from AEC, ASTU. He is an associate member of the Institution of Engineers (India). He has four book chapters, five international journal articles and a number of conference papers and posters to his credit. He has also acted as reviewer for reputed international journals and conferences. He is a recipient of many research awards in conference and conclaves, recognition, government project funding and scholarship. His research interest includes advanced manufacturing, microfabrication, solid lubrication, and microfluidics.

Dibya Jyoti Borah is currently working as the Deputy Manager (E/M) at the Kameng Hydro Electric Project, NEEPCO Ltd., Arunachal Pradesh, India. He received his Graduation in Mechanical Engineering from the Dibrugarh University and Master of Technology in Design and Manufacturing from National Institute of Technology Silchar, Assam. He is a recipient of MHRD GATE scholarship. He has one international journal article and international conference paper to his credit. His areas of interest include traditional and non-traditional machining. He has two years of teaching and five years of industrial experience.

Promod Kumar Patowari is currently serving as a Professor in the Department of Mechanical Engineering of National Institute of Technology (NIT) Silchar, Assam. He obtained his BTech in Mechanical Engineering from the North Eastern Regional Institute of Science and Technology (NERIST), Itanagar in 1994, MProdE in Production Engineering from Jadavpur University, Kolkata in 1999, and PhD from Indian Institute of Technology (IIT) Kharagpur in 2008. He has joined as a faculty member in the Department of Mechanical Engineering of National Institute of Technology (NIT) Silchar in 1995. He has published/presented a number of technical articles in reputed international journals and conferences. He is a life member of professional bodies like Indian Society for Technical Education (ISTE) and Institute of Smart Structures and Systems (ISSS). His research interest includes traditional and advanced machining, micro-nanofabrication, CAD/CAM and microfluidics.

Ajay Likhite is currently serving as an Associate Professor in the Department of Metallurgical and Materials Engineering, Visvesvaraya National Institute of Technology, Nagpur, Maharashtra, India. He received his BE in Metallurgy in 1983 and MTech in Ferro Alloys Technology and Alloy Steel Making, in 1985 from the Visvesvaraya Regional College of Engineering (VRCE), Nagpur and

PhD in Metallurgical and Materials Engineering in 2008 from VNIT Nagpur. He has published/presented a number of technical articles in reputed international journals and conferences. His areas of interests are austempered ductile iron, solidification processing, process control, Taguchi methods, foundry technology and failure analysis.

1 Introduction

The manufacturing sector is rapidly advancing and continuous demand for high quality product leads to the encounter of various materials having superior mechanical properties. Austempered ductile iron (ADI) falls under such advanced category of materials which is gaining interest as it posses many desirable material properties suitable for producing excellent quality products. ADI posses high strength (UTS ~ 1,000 MPa), high hardness (HRc ~ 50) and excellent toughness (Wang et al., 2019; Mussa et al., 2022). In addition to these, good ductility, high abrasion resistance, tunable damping properties, high strength with low weight, cost effectiveness, high resistivity to crash are some added bonus of ADI (Sarma et al., 2022; Sellamuthu et al., 2018; Böhme and Reissig, 2015; Fernández Scudeller and Martínez, 2016). Owing to these qualities, ADI makes an appropriate candidate and has found applications in structural, automotive, gear, rail as well as defence industries (Kumar et al., 2018; López de Lacalle et al., 2020). But the same strength and hardness properties also make ADI a very difficult to machine material, previously forming a myth about it to be non-machinable (Brandenberg, 2001). Bahmani et al. (1997) reported the possibility of replacing steel with ADI for crankshaft material with the added advantage of saving 10% in weight and 30% in cost. But machining of ADI still remains a challenging task, and conventional machining processes are not so suitable for it, and many a times demand specialised tools, cutting inserts and special attention (Arft and Klocke, 2013). Due to its suitability, ADI has even emerged as an alternative to traditional heavy grey cast irons, few aluminium alloys and steels for some applications (Polishetty, 2012; Fernández Scudeller and Martínez, 2016; Hegde et al., 2021). But still, its potentials remains underutilised and machining difficulty is one of the main factors hindering its wide spread applications. Proper understanding of its machining characteristics is thus very important for the advancement in the field of research and application of ADI.

Processing of hard to machine material like ADI via traditional method has drawbacks like direct contact of tool with work piece, high tool wear, noise, heat and vibration along with low dimensional accuracy (Hwang et al., 1997). Due to the transformation induced by strain, the tool life is greatly reduced in the conventional machining of ADI (Sharun and Ronald, 2022). Advanced machining methods like wire electric discharge machining (WEDM), die sinking electric discharge machining (EDM) can machine any material irrespective of their hardness as long as they are electrically conductive and highly suitable for precision machining of superalloys (Paulson et al., 2022; Singh et al., 2022). Even the machining happens without any actual contact between the tool and the work piece. Hence, ADI being electrically conductive can potentially be processed via WEDM. Apart from that, considering WEDM for ADI processing can also produce parts with complex geometry, superior surface finish with close dimensional tolerance and there is less residual stress on the machined parts

(Hwang et al., 1997). The various parameters influencing the quality of parts fabricated by WEDM process include peak current, pulse on time, pulse frequency, wire feed, dielectic flow rate, wire tension and flushing pressure (Khan et al., 2015). On the other hand, different performance measures of WEDM include kerf width, cutting rate (CR), surface roughness (SR) and edge sharpness. WEDM has been successfully employed to machine different traditional and advanced materials like stainless steel implant, H13 tool steel, AISI T-15-HSS, Ti-6Al-4V alloy, AISI H11 tool steel, maraging steel 300, gamma titanium aluminides, AISI D2 steel, Inconel 718, etc. among many others (Sivakumar et al., 2020; Sarma and Singh, 2020; Chockalingam et al., 2019; Sharma et al., 2019; Salamina et al., 2022; Sen et al., 2018; Vignesh and Ramanujam, 2018; Anurag, 2018; Dhobe et al., 2012; Dhale and Deshmukh, 2022). WEDM process is a comparatively fast machining process when considering processing of difficult to cut material and best suited for processing materials with poor machinability (Baburaj et al., 2022). Apart from cutting operations, WEDM has been successfully employed in micro domain for fabricating micro fin array, micro tools for microfluidic related applications (Debnath and Patowari, 2019; Sarma and Patowari, 2018, 2019).

From the literature, it is found that researchers have demonstrated processing of ADI via methods like EDM, gear shaping, milling, cylindrical grinding, etc. (Sarma et al., 2022; Kühn et al., 2021; López de Lacalle et al., 2020; da Silva et al., 2020). Some works are also available where the researchers have examined the effect of austempering parameters on the resultant ADI with respect to its mechanical properties and microstructure variation (Sellamuthu et al., 2018; Zhang et al., 2021; Uyar et al., 2022). It has been reported that the superior mechanical properties like high strength and hardness makes ADI difficult to machine. This necessitates exploring other non-traditional avenues like WEDM for machining ADI. Even though work exists on utilisation of WEDM in advanced fields like machining titanium-based human implant, nitinol shape memory alloy (Kumar et al., 2019; Liu et al., 2018), there is a very limited work available which focus to understand the machinability characteristics of ADI via WEDM. Hence, this work has been undertaken with an objective to better understand the WEDM machinability characteristics of developed ADI-4h material.

Mild steel (MS) is a very traditional and important material having various applications. Its tensile strength is relatively low but has high malleability and cheap (Khan et al., 2015). Though MS has been successfully processed using conventional machining methods, limited work has been done to understand its machinability characteristics using advanced machining processes like WEDM. In this work, the primary material under investigation is ADI-4h and MS has been selected with an objective to understand its machinability via WEDM as well as to compare machinability of developed ADI-4h with it. Here, we investigate the effect of peak current (I_P), pulse-on-time (T_{on}) and wire feed (W_f) which are three primary WEDM machining parameters on the response parameters viz. CR, kerf width (K_f) and SR while processing ADI-4h and MS via WEDM. Microstructure of the synthesised ADI-4h and recast layer formed during its processing has also been revealed via scanning electron microscope (SEM) micrograph analysis. The first section of the manuscript gives a general introduction with overview of the relevant literatures and the need of the work. The development process of ADI-4h and experimental methodology is explained in the second section. The subsequent sections discuss the various results obtained from the experiments and the conclusions drawn from the study.

2 Materials and methods

2.1 ADI-4h and MS

ADIs fall under high carbon ferrous material (Mussa et al., 2022). Based on the broad spectrum of strength and hardness, there exist six ASTM standard grades of ADI. Heat treatment under tight process controlling is the key to achieve the unique microstructure desired in ADIs imparting its ductility as well as strength and hardness features. Nodular graphite which is present in the ADI matrix inhibits the crack formation as there is no stress concentration point in contrast to their flake shaped counterparts. The unique material properties associated with ADI has made it an important material. ADI production via austempering is an isothermal heat treatment process comprising of many stages. Initially, the casting is heated to the austenising temperature where it is held with an objective to obtain carbon saturated austenite. Quenching the job to austempeing temperature is done next followed by austempering for sufficient time to produce the special microstructure desired. Properly maintaining the austempering time is important to inhibit carbide formation towards the later stage of austempering which otherwise makes the ADI brittle. Table 1 shows the % weight of various constituent elements of the ADI material under investigation. Initially, austenisation of the ADI to 900°C has been done, which is later allowed to cool to an austempering temperature of 250°C and held for four hour to achieve the resultant properties. Hence, the work material is designated as ADI-4h, the austempering specifications and property of which are listed in Table 2.

Table 1 ADI-4h composition

Alloying element	*C*	*Si*	*Ni*	*Cu*	*Mn*
% weight	3.36	2.95	0.767	0.598	0.4

Table 2 Austempering specifications of ADI-4h

Material	*Austenising temperature*	*Austempering temperature*	*Austempering time*	*Hardness (BHN)*
ADI-4h	900°C	250°C	4 hour	340

Table 3 Properties of MS work piece

Material	*Electrical conductivity*	*Thermal conductivity*	*Melting point*
MS	6.99×10^6 S/m	54 W/(m.K)	1,425°C

Another work material considered for the comparison purpose is commonly available MS of dimension 50 mm × 50 mm × 5 mm. Both the work materials are pre cleaned for conducting experiments. Some material properties of the MS work piece are listed in Table 3.

2.2 Experimental setup and procedure

In WEDMm electrical energy is utilised to produce complex and simple 2D/3D profiles on electrically conductive work piece which essentially is a spark erosion process. Here, a very small diameter wire is used as the tool electrode. A series of discrete electric discharges generating in the gap between the wire electrode and the work piece cuts the

material. The spark gap is flooded with a dielectric fluid. Generally, a localised dielectric fluid stream is used here unlike in conventional die sinking type of EDM, which flushes away any debris produced during the cutting process. Schematics of WEDM setup and a straight cut by WEDM showing the kerf and the spark gap ahead of the wire are shown in Figure 1.

Figure 1 (a) Schematic diagram of WEDM setup (b) A straight cut showing the kerf and spark gap (see online version for colours)

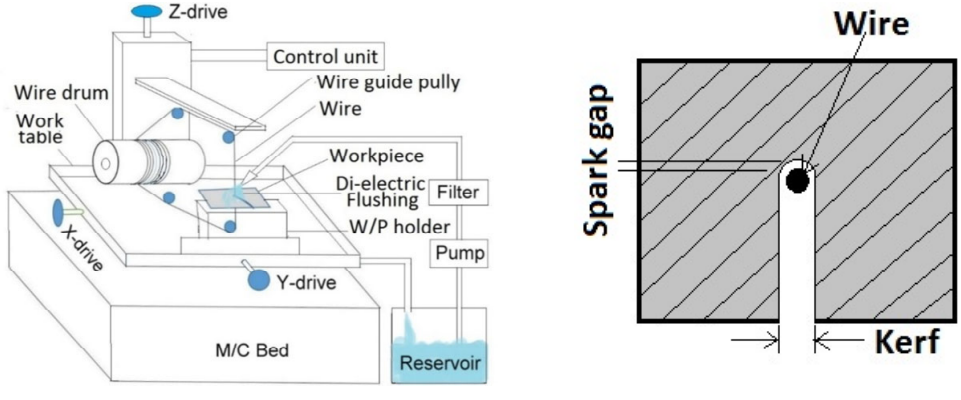

(a) (b)

The relative travelling of the wire over the work piece defines the cutting path. Computer numerical control (CNC) is used for this purpose which generates a very precise cutting. During the process, the wire is un-winded from a spool, fed through the work piece and taken back on the same or different spool. High frequency electrical pulses are delivered to both the electrodes (tool and work piece) via a DC power supply. Erosion of material ahead of the travelling wire takes place by spark discharges which generates very high temperature and melts the work piece. A continuous stream of dielectric at the working zone flushes away the eroded particles and also cools the work piece. Proper flushing is important to ensure stable discharging by effective exclusion of debris as the spark generation area is very narrow in WEDM (Kimura et al., 2022). As reported by Wang et al. (2022), a lower flushing pressure can make early occurrence of discharge by minimising the delay time of discharge. Non-contact between the tool wire and the work piece is ensured by maintaining a definite gap between the two by CNC unit. These allow WEDM to accurately cut any hard to machine material provided it is electrically conductive.

In this investigation, the machining has been done in CNC Ezeewin WEDM (make: Ratnapakhi (I) Pvt. Ltd., model: Ezeecut NXG). The tool used is a brass wire whose diameter ranges within the limit of 200–250 µm. Brass wire is selected because as compared to copper wires it possesses good conductivity alongside high tensile strength (Khan et al., 2015). Also, brass wire has shown better achievable surface smoothness during finish cuts compared to copper wire (Günen et al., 2022). The dielectric used is a mixture of deionised water with S100 coolant in a ratio of 40:1. Use of deionised water as dielectric is conventional in WEDM (Liu et al., 2022). Leica (model: DM 2500M) metallurgical microscope is used to measure the kerf widths and a Handysurf profilometer is used for SR evaluation. For evaluation of the CR, the cutting time

displayed on the WEDM display unit has been used. The CR is expressed by equation (1).

$$\text{CR} = \frac{\text{length of cut}}{\text{cutting time}} \tag{1}$$

The flow diagram of the machining steps involved during the machinability study of ADI using WEDM is shown in Figure 2. Initially from the developed ADI-4h bar stock, 5 mm thick slices are cut which act as the work piece for the experiments. Slots are cut on the work piece via WEDM under various parametric conditions and then different response parameters viz. CR, K_f and SR are evaluated. Slots of same length (10 mm) under similar parametric conditions have been cut on the prepared MS specimen for the comparison purpose.

Figure 2 Machining procedure (see online version for colours)

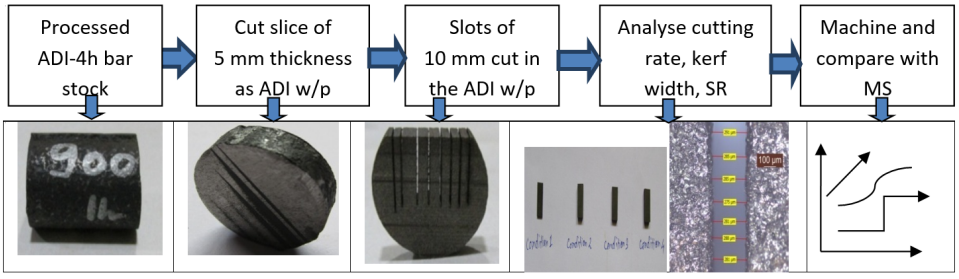

Table 4 WEDM parameters and their values at different levels

Parameters	*Level 1*	*Level 2*	*Level 3*	*Level 4*
Peak current (A)	1	2	3	4
Pulse-on-time (μs)	10	20	30	40
Wire feed (mm/s)	60	70	80	90

For the machinability investigation, each of the machining parameters selected are varied in four levels as enlisted in Table 4. For the selection of the range of machining parameter for this study, a number of initials pilot experiments have been conducted and available literature is consulted (Tilekar et al., 2014; Debnath and Patowari, 2019). Based on that, the variable parameters considered for investigation are – I_P, T_{on} and W_f. Other factors like wire material, wire tension, duty factor, dielectric flushing pressure, length of cut and sensitivity are kept constant during the experiments. Duty factor is maintained around the range of 60%–70% using the available parametric values from the WEDM setup.

3 Results and discussion

Here, we present a comparative machinability study of ADI-4h and MS under wire-EDM. The machining performance of both the materials at same parametric condition has been evaluated and compared. The effect of I_P, T_{on} and W_f on CR, K_f and SR are reported on

the subsequent sections. For the experimentation and reporting, one factor at a time approach has been considered. All the experiments are conducted a number of times and the average of those results is reported.

3.1 Effect of I_P

I_P is an important machining parameter affecting WEDM process performance. I_P indicates the discharge energy that is needed to melt and vaporise the material under process. Here, the I_P is varied at four levels viz. 1 A, 2 A, 3 A and 4 A. T_{on} and W_f are kept constant at 20 µs and 80 mm/s, respectively. A lower level value of T_{on} has been selected so that the effect of the parameter under investigation becomes dominant. Also, the W_f value is selected as the average of the two optimum values reported by Tilekar et al. (2014).

3.1.1 Effect of I_P on CR

From Figure 3, it is seen that in general CR shows an increasing trend with increase in I_P. This may be attributed to the fact that each spark at higher I_P is associated with increased sparking energy and heat concentration. This facilitates removal of larger crater per spark. It is the probable occurrence of arcing between the two electrodes at higher value of I_P which results in a decrease in CR. For both the materials, initially the CR is seen to increase with I_P and then it decreases for higher I_P. MS being a comparatively softer material provides a higher CR than ADI except at a higher I_P (4 A). Highest CR obtained at I_P = 3 A for ADI-4h and MS are 7.32 and 7.79 mm/min, respectively.

Figure 3 Comparison of effect of I_P on CR for ADI and MS (see online version for colours)

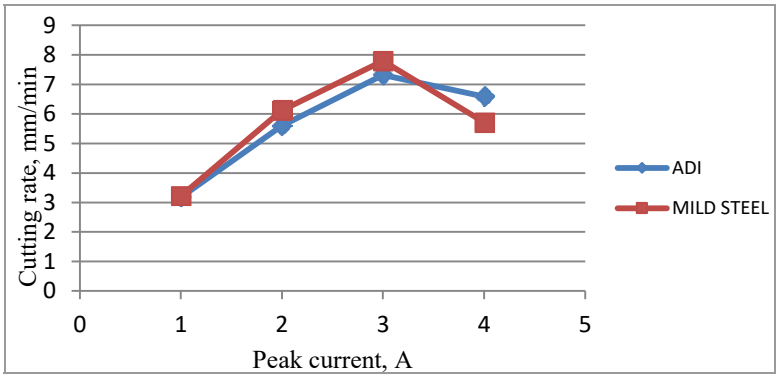

3.1.2 Effect of I_P on K_f

From Figure 4, it is evident that as I_P increases the K_f increases, but it decreases again at the highest level of I_P. Higher I_P results in higher spark energy producing deeper cavity on the surface, which in turn increases the K_f. But at the highest I_P, there is possibility of arc occurrence between the electrodes. This may be due to the condition of stray molten material remaining un-flushed by the dielectric and re-deposition on the work surface. This leads to the reduced kerf width. It can be seen that the trend is similar for both the materials. MS has a higher K_f than ADI except at highest I_P level. The profiles of the

kerfs at different I_P are shown in Figure 5. It is needless to reaffirm that the minimum kerf width attainable is always greater than the wire diameter at any given parametric combination.

Figure 4 Comparison of the effect of I_P on K_f for ADI and MS (see online version for colours)

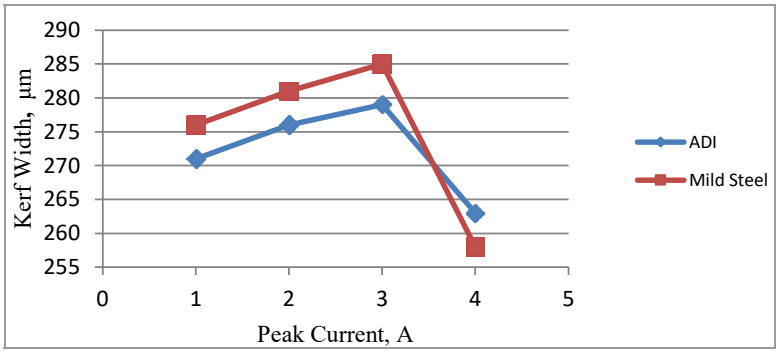

Figure 5 Kerf profiles of ADI and MS at various I_P (see online version for colours)

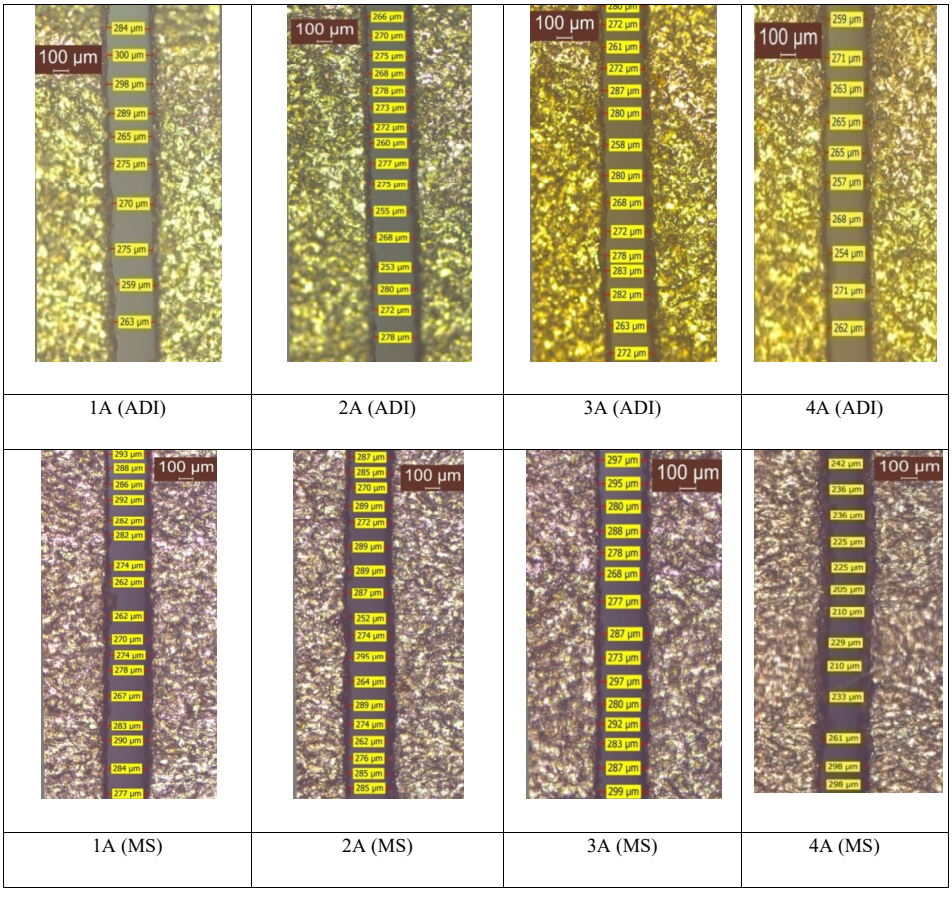

Figure 6 Comparison of effect of I_P on SR for ADI and MS (see online version for colours)

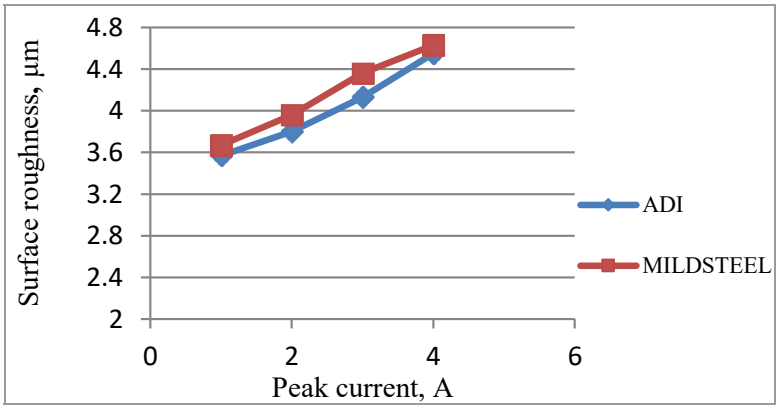

Figure 7 A typical SR profile for ADI-4h (see online version for colours)

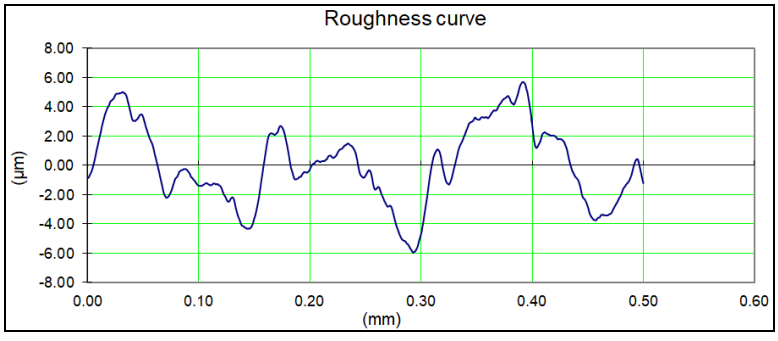

3.1.3 Effect of I_P on SR

Figure 6 shows increase in SR when I_P increases. The higher discharge energy at higher I_P produces craters of bigger size. These increase the undulation in the machined surface resulting in higher SR. It can be observed that the trend for both the materials is same. The MS has higher SR than ADI. The minimum SR is achieved at the lowest level of I_P = 1 A and yielding values of 3.57 and 3.67 µm for ADI and MS, respectively. A typical representative SR profile is shown in Figure 7.

3.2 Effect of T_{on}

T_{on} is the time for which there is discharge of energy within a cycle which comprises of pulse on and off time. The ratio of pulse on time to the cycle time gives an important factor known as the duty factor as given by equation (2).

$$\text{Duty factor} = \frac{T_{on}}{T_{on} + T_{off}} \tag{2}$$

For the experimentation purpose, T_{on} is varied at four levels viz. 10, 20, 30 and 40 µs for both the materials and their effect on the response parameters are studied individually. I_P

and W_f are kept constant with a parametric setting of I_P = 2 A and W_f = 80 mm/s, respectively. A lower level value of I_P has been selected to ensure that the effect of the parameter under investigation becomes dominant. Same W_f as that of the previous study is considered.

Figure 8 Comparison of effect of T_{on} on CR for ADI and MS (see online version for colours)

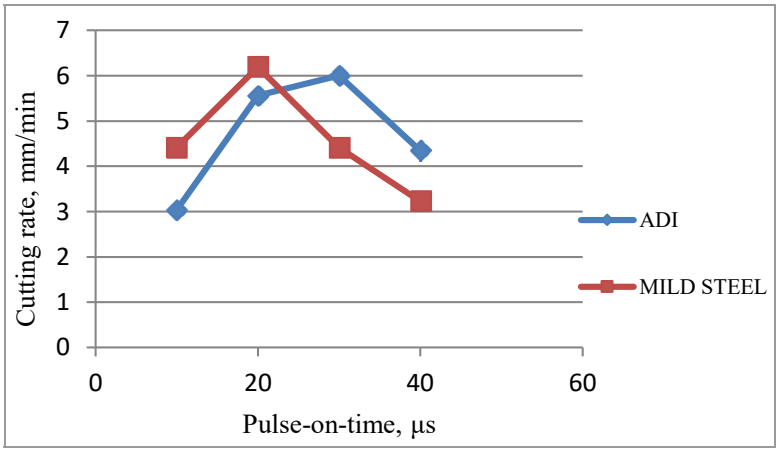

3.2.1 Effect of T_{on} on CR

Figure 8 shows that an increase in T_{on} increases the CR in case of ADI and then after T_{on} = 30 µs, CR is seen to decrease. But in MS, the decrease in CR is prior; as the CR decreases with T_{on} after 20 µs. MS provides a higher CR at T_{on} almost below 20 µs, but at higher T_{on} ADI provides higher CR. Initially, CR increases with the increasing T_{on}. The effective duration of sparking increases with increase in T_{on} which makes higher sparking energy available per cycle. This facilitates increased removal of material. In case of longer T_{on}, there is a possibility of expansion of the plasma channel, thereby decreasing the available energy density on the work part. The energy density may become inadequate for effective material removal and decreases the CR. Frequent retraction of the electrode due to higher risk of short-circuiting or arcing at higher T_{on} may also lead to decrease in the CR.

3.2.2 Effect of T_{on} on K_f

For both the materials, K_f increases with increase in T_{on}, however at higher T_{on}, the K_f slightly decreases as can be seen from Figure 9. This may be due to the re-solidification of the molten material at that level. MS mostly has a higher K_f than ADI owing to the softer nature of MS. At low T_{on}, low discharge energy of the spark produces shallow craters resulting in lesser K_f. Again at a higher T_{on} re-solidified of molten material happens on the surface as the bigger sized debris was not effectively flushed away within the small time. This again decreases the K_f. The kerf profiles at different T_{on} are shown in Figure 10. The minimum K_f values which are obtained at the lowest level of T_{on} are 247 and 262 µm for ADI and MS, respectively.

Figure 9 Comparison of effect of T_{on} on K_f for ADI and MS (see online version for colours)

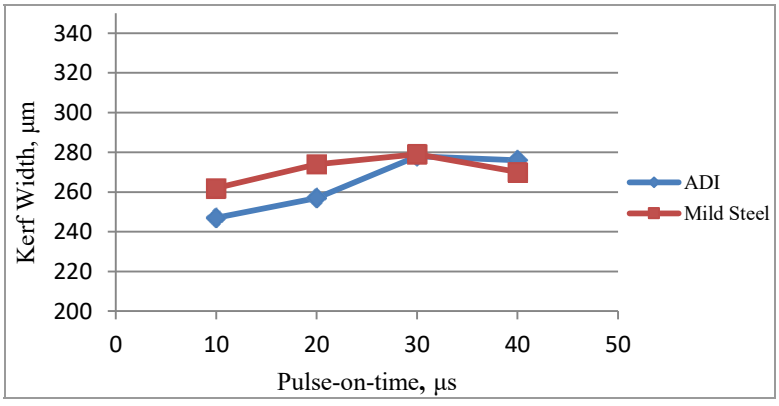

Figure 10 Kerf profiles of ADI and MS for various T_{on} (see online version for colours)

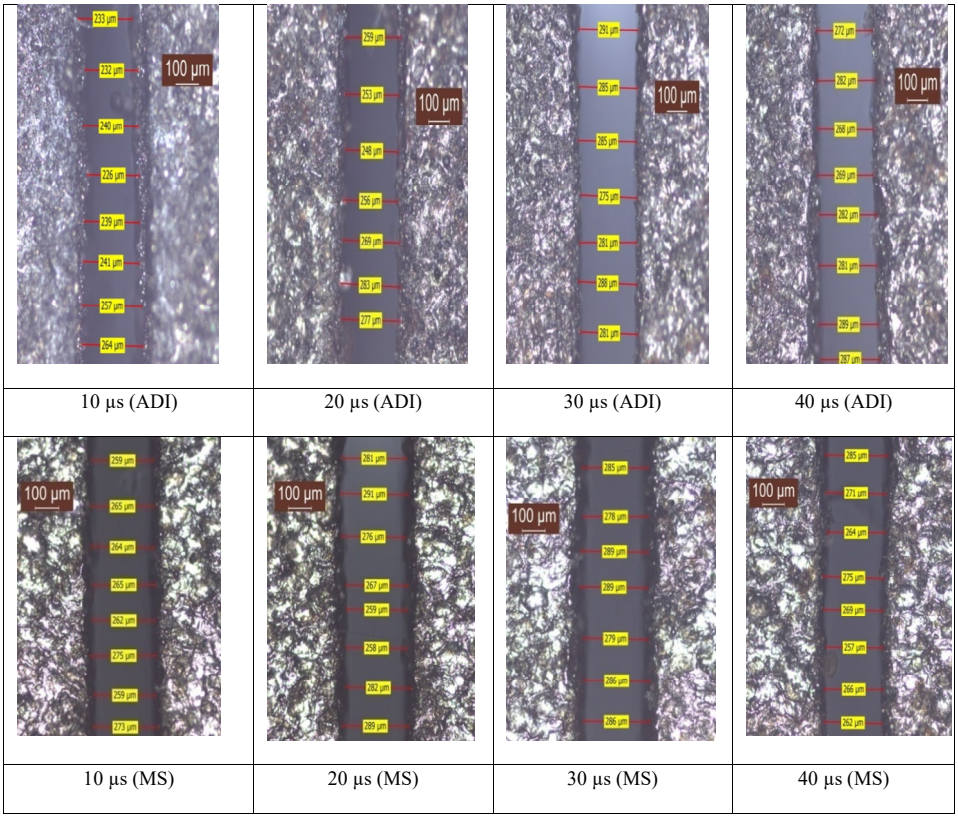

10 µs (ADI)	20 µs (ADI)	30 µs (ADI)	40 µs (ADI)
10 µs (MS)	20 µs (MS)	30 µs (MS)	40 µs (MS)

3.2.3 Effect of T_{on} on SR

It is seen from Figure 11 that increase in T_{on} also increases the SR, which is primarily due to the larger craters produced by the increased number of effective sparks. It can be seen

that the SR varies significantly with respect to the T_{on}. For both the materials the SR achieved has less difference, with ADI producing better surface. The minimum roughness values which are achieved at the lowest level of T_{on} with other constant parametric conditions are 3.32 and 3.58 µm respectively for ADI and MS.

Figure 11 Comparison of effect of T_{on} on SR for ADI and MS (see online version for colours)

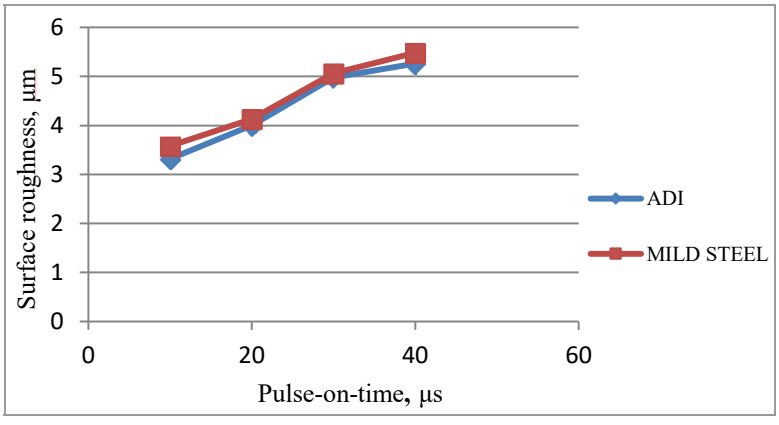

3.3 Effect of W_f

Here, the W_f is varied at four levels viz. 60, 70, 80 and 90 mm/s. Constant I_P and T_{on} of 2 A and 20 µs respectively are utilised during these experiments, which are kept same as that of the previous studies.

Figure 12 Comparison of effect of W_f on CR for ADI and MS (see online version for colours)

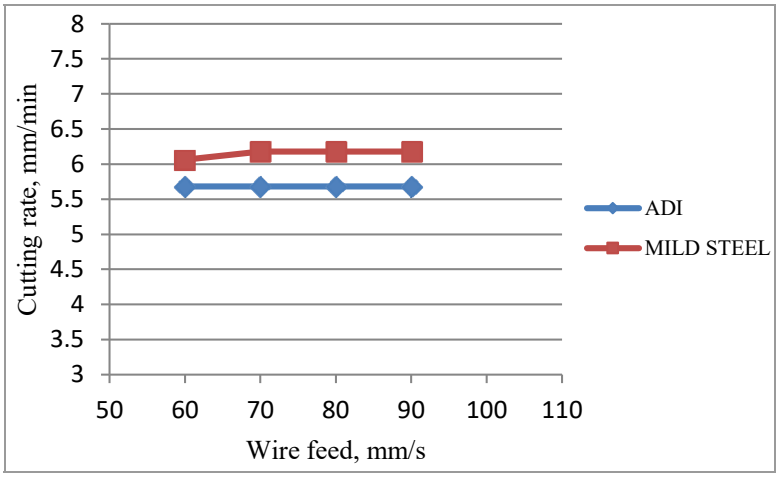

3.3.1 Effect of W_f on CR

It has been observed that there is almost no influence of W_f on CR within the machining range. Hence, it is recommended to keep the W_f at low/medium level to reduce wire consumption and enhance the process economics. MS provides a higher CR than ADI for the same W_f, which is expected because ADI has more strength than MS. While there is no fluctuation of CR obtained for ADI during the cutting of the constant length slot considered in the study; a very minimal increase in the CR was seen for MS at the higher levels which remained unchanged afterwards as can be seen from Figure 12.

3.3.2 Effect of W_f on K_f

With increase in W_f, the K_f increases for both the materials as evident from Figure 13. It may be attributed to the fact that increasing W_f leads to more machining happening at the same area of cut. This in turn leads to removal of more material and hence a bigger kerf is resulted. The kerf profiles at various W_f are shown in Figure 14. For all the levels, the kerf width in case of MS is found to be more as compared to ADI.

Figure 13 Comparison of effect of W_f on K_f for ADI and MS (see online version for colours)

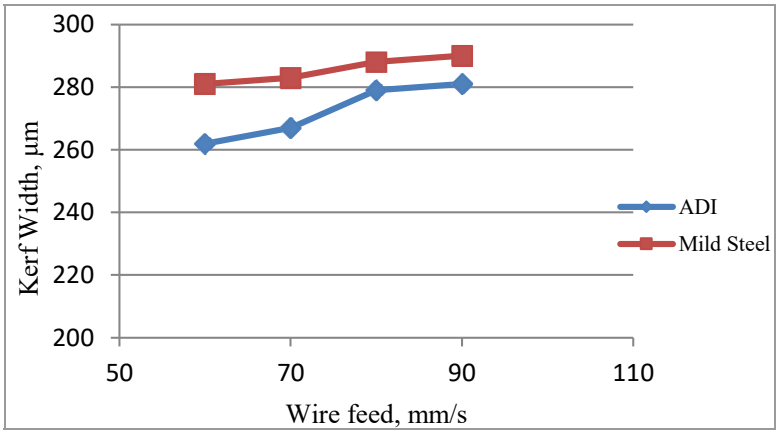

3.3.3 Effect of W_f on SR

Figure 15 shows the effect of W_f on SR for both the materials. It can be seen that SR for both the materials increase with the increase in W_f and it shows an almost linear trend. The maximum variation of roughness is only 0.59 µm. MS is seen to have higher SR than ADI.

From this machinability study, it can be concluded that MS shows higher CR in WEDM than ADI, but the surface finish is poor in MS and K_f is more in case of MS. It can be observed that I_P and T_{on} are the most important process parameters affecting the performance of machining. The effect of W_f is very small. With increase in I_P and T_{on}, the CR increases but the SR deteriorates.

Figure 14 Kerf profiles for ADI and MS at various W_f (see online version for colours)

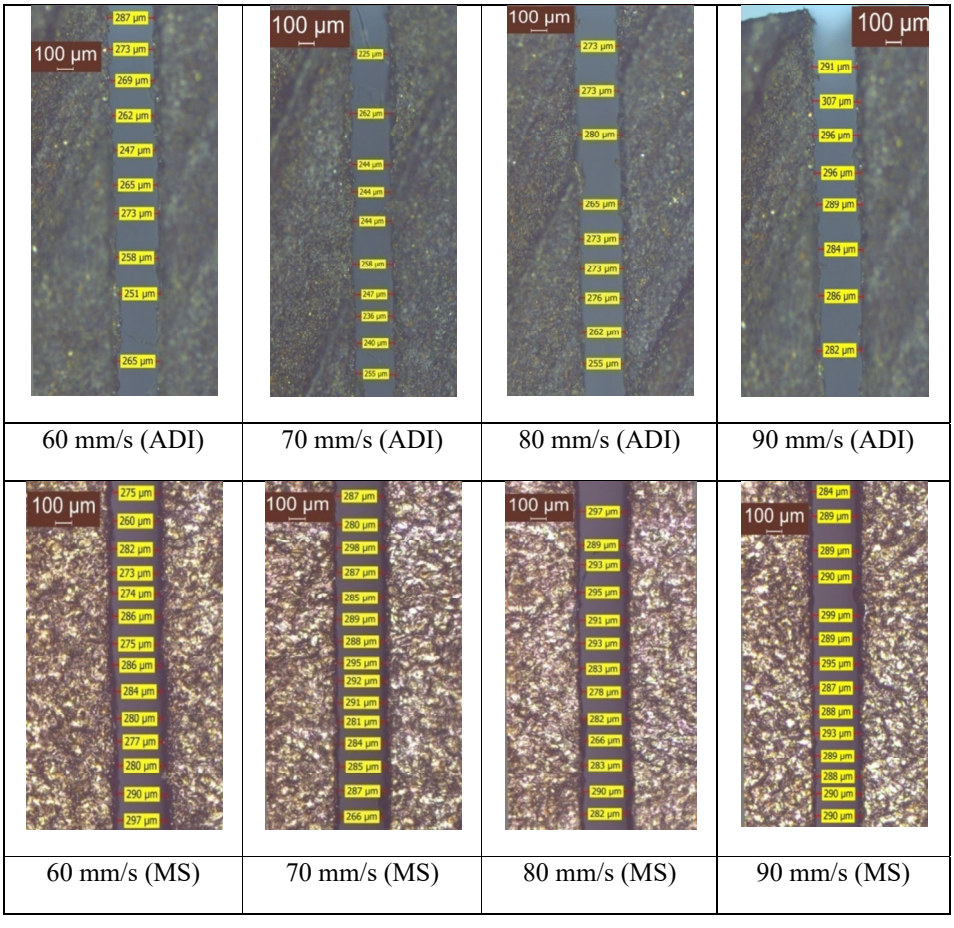

Figure 15 Comparison of effect of W_f on SR for ADI and MS (see online version for colours)

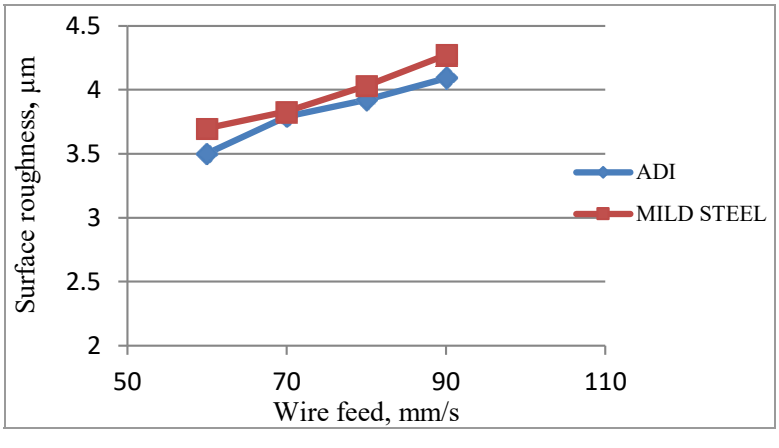

3.4 Microstructure of ADI-4h

The microstructure of ADI-4h contains nodular graphite particles scattered over the matrix. Nodular graphite particles can be seen embedded in the matrix of ADI-4h from Figure 16(a). Carbides are not apparent in ADI-4h which could be seen in ADI-7h due to disintegration of austenite towards final stages of austempering (Sarma et al., 2022). The ADI-4h shows the typical ausferritic matrix as evident from Figure 16(b). Better ductility and fatigue resistance in ADI is a typical result associated with this microstructure (Daniel et al., 2020).

Figure 16 Microstructure of ADI-4h, (a) graphite molecules embedded in the matrix in the form of nodules in ADI-4h (b) typical ausferritic matrix in ADI-4h

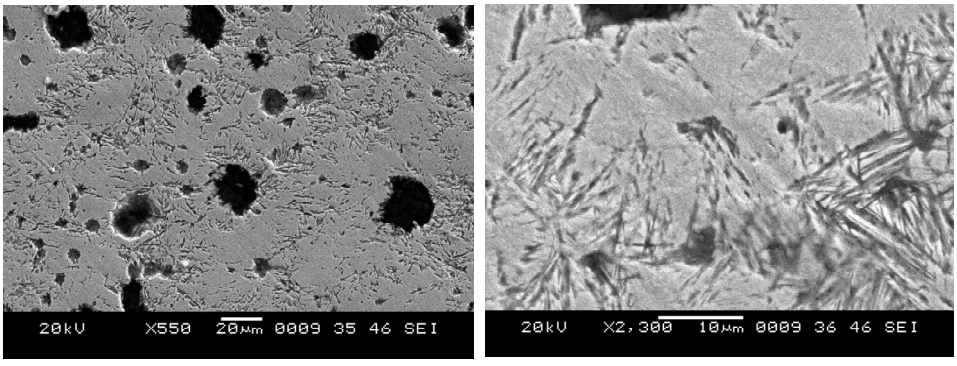

(a) (b)

Figure 17 SEM images showing recast layer formation on the machined surface of ADI-4h

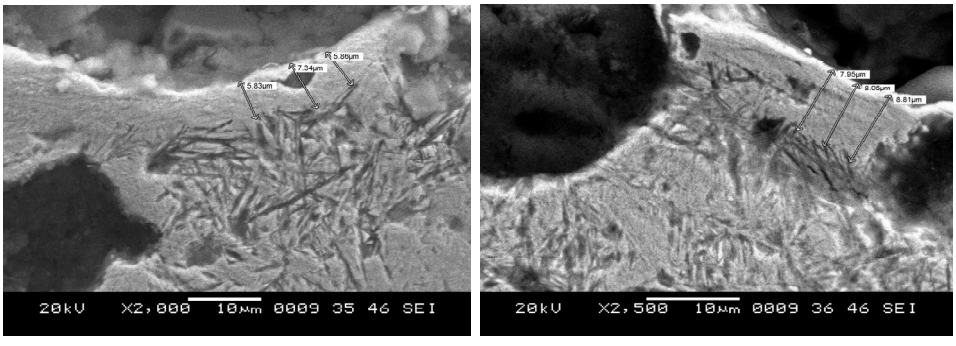

3.5 Recast layer in ADI-4h

A recast layer is a layer which is generated on the machined surface due to the quick re-solidification of the molten materials during WEDM. It is also known as white layer. Recast layer formation in work parts processed by WEDM is a typical phenomenon. “The recast layer is formed at a cooling rate lower than that at the outer surface, where the melted material is resolidified very quickly without having any grain boundaries” (Pramanik et al., 2021). The formation of recast layer may also be attributed to

inadequate flushing allowing setting of resolidified material on the part. The formation of the recast layer enhances the surface hardness but at the same time makes it more brittle. ADI-4h being the primary material under investigation, two representative SEM images of recast layers produced for ADI-4h at two different places of the machined surface under two different magnification levels are shown in Figure 17. Analysis of the SEM images has revealed formation of recast layer for ADI-4h with an average thickness of ~ 6 μm.

4 Conclusions

ADI being superior quality metal is difficult to machine via conventional route. Here, we present a comparative study of the machinability of ADI-4h and MS under WEDM. The machining responses are greatly affected by the machining parameters. The following are the main conclusions drawn from this study:

- WEDM can be implemented to effectively machine ADI-4h which has shown a good machinability under the investigated parametric range. MS is more easily machinable due to its softer nature. Proper selection of parametric combination is an important factor while processing via WEDM.
- Increase in I_P increases all the response measures viz. CR, K_f and SR. But CR is observed to decrease again at a higher value of I_P. Maximum CR recorded is 7.32 mm/min at 3 A. The K_f first increases with increase in I_P and then decreases at higher value of I_P due to larger extent of re-solidification of the molten material. The SR increases with increase in I_P due to the larger sized craters produced at higher I_P. The SR varies from 3.57 μm to 4.55 μm for a variation of I_P from 1 A to 4 A.
- As the T_{on} increases the CR increases and then again decreases for higher value of T_{on}. The highest CR obtained was 6 mm/min at a T_{on} of 30 μs. The K_f first increases and then decreases with T_{on}. The minimum K_f of 247 μm was obtained at a T_{on} of 10 μs and the maximum value of K_f was 278 μm at 30 μs. The SR increases significantly from 3.32 μm to 5.26 μm for a variation of T_{on} from 10 μs to 40 μs.
- W_f is least significant in affecting the machining performance compared to the other two investigated parameters. The W_f does not have any appreciable influence on the CR. A constant CR of 5.80 mm/min was obtained for all of the four wire feeds. The K_f and the SR increase with the increase in W_f, but it is the least influencing among the parameters.
- Comparison of machinability of ADI-4h with MS reveals that during the variation of I_P, T_{on} and W_f, the trend of the effect of these parameters on the machining responses is almost similar for both the materials. MS provides a higher CR than ADI. K_f is more in case of MS. The minimum K_f obtained in ADI and MS were 247 μm and 258 μm, respectively. ADI has a better surface finish than MS.
- The microstructure of ADI-4 hour is found to be a mixture of acicular bainitic ferrite and carbon enriched austenite that provides better ductility as well as fatigue resistance.

- SEM analysis reveals formation of a thin recast layer in ADI-4h which is a typical feature of WEDM processed parts. An average recast layer thickness of ~ 6 μm has been seen.

This work has shown that WEDM can be implemented to process ADI successfully. It is expected that this work will advance the field of ADI application in newer areas which were previously less explored due to the processing difficulties of ADI. With the ability of fabricating intrinsic details by WEDM and the superior material property advantage to be gained by shifting to ADI; ADI is bound to take the manufacturing industry by storm.

References

Anurag, S. (2018) 'Wire-EDM: a potential manufacturing process for gamma titanium aluminides in future aero engines', *International Journal of Advance Manufacturing Technology*, Vol. 94, Nos. 1–4, pp.351–356.

Arft, M. and Klocke, F. (2013) 'High performance turning of austempered ductile iron (ADI) with adapted cutting inserts', *Procedia CIRP*, Vol. 8, pp.129–134, https://doi.org/10.1016/j.procir.2013.06.077.

Baburaj, M., Kumar, K.M., Mathew, N.T. and Nathan, S.R. (2022) 'A novel approach to measure kerf-width in wire-electric discharge machining', *International Journal of Machining and Machinability of Materials*, Vol. 24, No. 5, pp.331–349.

Bahmani, M., Elliott, R. and Varahram, N. (1997) 'Austempered ductile iron: a competitive alternative for forged induction-hardened steel crankshafts', *International Journal of Cast Metals Research*, Vol. 9, No. 5, pp.249–257.

Böhme, W. and Reissig, L. (2015) 'Capability of new high strength ADI-materials for automotive components under crash loading: capability of new high strength ADI-materials', *Advanced Engineering Materials*, Vol. 17, No. 8, pp.1189–1196.

Brandenberg K. (2001) *Successfully Machining Austempered Ductile Iron (ADI)* [online] https://www.appliedprocess.com/wp-content/uploads/2018/09/233948_Machining-ADI-final-revision.pdf (accessed 12 September 2022).

Chockalingam, K., Jawahar, N., Muralidharan, N. and Jeyaraj K.L. (2019) 'Material subtraction study of AISI T-15-HSS by wire cut electrical discharge machining (CNC-wire cut EDM) based on Taguchi grey relational analysis', *International Journal of Machining and Machinability of Materials*, Vol. 21, No. 3, pp.139–168.

da Silva, A.E., Lopes, J.C., Daniel, D.M., de Moraes, D.L., Garcia, M.V., Ribeiro, F.S.F., de Mello, H.J., Sanchez, L.E.D.A., Aguiar, P.R. and Bianchi, E.C. (2020) 'Behavior of austempered ductile iron (ADI) grinding using different MQL dilutions and CBN wheels with low and high friability', *The International Journal of Advanced Manufacturing Technology*, Vol. 107, Nos. 11–12, pp.4373–4387.

Daniel, D.M., Ávila, B.N., Garcia, M.V., Lopes, J.C., Ribeiro, F.S.F., Mello, H.J., Sanchez, L.E.D.A., Aguiar, P.R. and Bianchi, E.C. (2020) 'Grinding comparative between ductile iron and austempered ductile iron under CBN wheel combined to abrasive grains with high and low friability', *The International Journal of Advanced Manufacturing Technology*, Vol. 109, Nos. 9–12, pp.2679–2690.

Debnath, T. and Patowari, P.K. (2019) 'Fabrication of an array of micro-fins using wire-EDM and its parametric analysis', *Materials and Manufacturing Processes*, Vol. 34, No. 5, pp.580–589.

Dhale, S.R. and Deshmukh, B.B. (2022) 'WEDM with different diameter wire electrodes on Inconel 718: improved dimensional deviation, wire consumption and surface quality', *Materials Today: Proceedings* [online] https://doi.org/10.1016/j.matpr.2022.09.088.

Dhobe, M.M., Chopde, K. and Gogte, C.L. (2012) 'Effect of heat treatment on the surface characteristics of AISI D2 steel machined by wire EDM', in Hwang, J.Y. et al. (Eds.): *Characterization of Minerals, Metals, and Materials*, pp.495–502, John Wiley & Sons, Inc., Hoboken, NJ, USA.

Fernández Scudeller, F. and Martínez, R.A. (2016) 'Evaluation of environmentally assisted fracture of austempered ductile iron (ADI) under cyclic load bearing: EAC under cyclic loads', *Fatigue and Fracture of Engineering Materials and Structures*, Vol. 39, No. 3, pp.346–356.

Günen, A., Ceritbinmez, F., Patel, K., Akhtar, M.A., Mukherjee, S., Kanca, E. and Karakas, M.S. (2022) 'WEDM machining of MoNbTaTiZr refractory high entropy alloy', *CIRP Journal of Manufacturing Science and Technology*, August, Vol. 38, pp.547–559, https://doi.org/10.1016/j.cirpj.2022.05.021.

Hegde, A., Gurumurthy, B.M., Hindi, J., Sharma, S. and Gowrishankar, M.C. (2021) 'Effect of austempering temperature and manganese content on the impact energy of austempered ductile iron', *Cogent Engineering*, Vol. 8, No. 1, p.1939928.

Hwang, L.R., Hwang, L.W., Chang, G.C. and Shih, T.S. (1997) 'Electrical-discharge wire cutting of ADI and its effect on impact energies', *International Journal of Cast Metals Research*, Vol. 10, No. 2, pp.105–116.

Khan, A.A., Al Hazza, M.H.F., Daud, M.R.H.C. and Kamal, N.S.B.M. (2015) 'Optimization of surface quality of MS machined by wire EDM using simulated annealing algorithm', in *2015 4th International Conference on Advanced Computer Science Applications and Technologies (ACSAT)*, IEEE, Kuala Lumpur, Malaysia, pp.3–8.

Kimura, S., Iwai, H., Liu, S., Okada, A. and Kurihara, H. (2022) 'Influence of nozzle jet flushing in wire EDM of workpiece with stepped thickness', *Procedia CIRP*, Vol. 113, pp.149–154 [online] https://doi.org/10.1016/j.procir.2022.09.123.

Kühn, F., Brimmers, J. and Bergs, T. (2021) 'Process design for gear shaping of austempered ductile iron (ADI) components', *Procedia CIRP*, Vol. 99, pp.214–219, https://doi.org/10.1016/j.procir.2021.03.098.

Kumar, K.M., Hariharan, P. and Ramesh, B. (2018) 'Study on the influential process parameters in machining the austempered ductile iron', *Materials and Manufacturing Processes*, Vol. 33, No. 4, pp.414–421.

Kumar, S., Khan, M.A. and Muralidharan, B. (2019) 'Processing of titanium-based human implant material using wire EDM', *Materials and Manufacturing Processes*, Vol. 34, No. 6, pp.695–700.

Liu, J.F., Li, C., Fang, X.Y., Jordon, J.B. and Guo, Y.B. (2018) 'Effect of wire-EDM on fatigue of nitinol shape memory alloy', *Materials and Manufacturing Processes*, Vol. 33, No. 16, pp.1809–1814.

Liu, S., Kimura, S., Okada, A. and Kitamura, T. (2022) 'Optimization of dielectric oil viscosity for high-precision wire EDM', *Procedia CIRP*, Vol. 113, pp.244–249 [online] https://doi.org/10.1016/j.procir.2022.09.153.

López de Lacalle, L.N., Fernández Valdivielso, A., Amigo, F.J. and Sastoque, L. (2020) 'Milling with ceramic inserts of austempered ductile iron (ADI): process conditions and performance', *The International Journal of Advanced Manufacturing Technology*, Vol. 110, Nos. 3–4, pp.899–907.

Mussa, A., Krakhmalev, P. and Bergstrom, J. (2022) 'Wear mechanisms and wear resistance of austempered ductile iron in reciprocal sliding contact', *Wear*, 15 June, Vols. 498–499, p.204305, https://doi.org/10.1016/j.wear.2022.204305.

Paulson, D.M., Saif, M. and Zishan, M. (2022) 'Optimization of wire-EDM process of titanium alloy-Grade 5 using Taguchi's method and grey relational analysis', *Materials Today: Proceedings* [online] https://doi.org/10.1016/j.matpr.2022.06.376.

Polishetty, A. (2012) *Machinability and Microstructural Studies on Phase Transformations in Austempered Ductile Iron*, PhD thesis, Auckland University of Technology, Auckland, New Zealand.

Pramanik, A., Basak, A.K., Prakash, C., Shankar, S., Sharma, S. and Narendranath, S. (2021) 'Recast layer formation during wire electrical discharge machining of titanium (Ti-Al6-V4) alloy', *Journal of Materials Engineering and Performance*, Vol. 30, No. 12, pp.8926–8935.

Salamina, S., Crivelli, D., Diviani, L., Berto, F. and Razavi, S.M.J. (2022) 'Strain energy density approach as fatigue assessment of Ti6Al4V specimens machined by WEDM single step technology', *International Journal of Fatigue*, August, Vol. 161, p.106915, https://doi.org/10.1016/j.ijfatigue.2022.106915.

Sarma, D.K. and Singh M.A. (2020) 'Machining of thin sections using multi-pass wire electrical discharge machining process', *International Journal of Machining and Machinability of Materials*, Vol. 22, No. 1, pp.62–78.

Sarma, P. and Patowari, P.K. (2018) 'Fabrication of metallic micromixers using WEDM and EDM for application in microfluidic devices and circuitries', *Micro and Nanosystems*, Vol. 10, No. 2, pp.136–146.

Sarma, P. and Patowari, P.K. (2019) 'Alternate soft lithographic approaches for microfluidic device fabrication using PCM and EDM based tools', in Kakati, B. et al. (Eds.): *Advances in Science and Technology*, Vol. 1, pp.1–5, i-Manager Publications, Tamil Nadu, ISBN: 978-81-908910-9-7.

Sarma, P., Borah, D.J., Patowari, P.K. and Likhite, A. (2022) 'Machinability study of austempered ductile iron using die-sinking EDM', *International Journal of Machining and Machinability of Materials*, Vol. 24, Nos. 3/4, pp.314–329.

Sellamuthu, P., Samuel, D.G.H., Dinakaran, D., Premkumar, V.P., Li, Z. and Seetharaman, S. (2018) 'Austempered ductile iron (ADI): influence of austempering temperature on microstructure, mechanical and wear properties and energy consumption', *Metals*, Vol. 8, No. 1, p.53.

Sen, R., Choudhuri, B., Barma, J.D. and Chakraborti, P. (2018) 'Experimental investigation and optimisation of WEDM process for machining maraging steel using neural network based Jaya algorithm', *International Journal of Machining and Machinability of Materials*, Vol. 20, No. 4, pp.387–399.

Sharma, N., Khanna, R., Sharma, Y.K. and Gupta, R.D. (2019) 'Multi-quality characteristics optimisation on WEDM for Ti-6Al-4V using Taguchi-grey relational theory', *International Journal of Machining and Machinability of Materials*, Vol. 21, Nos. 1/2, pp.66–81.

Sharun, V. and Ronald, B.A. (2022) 'Traditional machining of austempered ductile iron (ADI): a review', *Materials Today: Proceedings* [online] https://doi.org/10.1016/j.matpr.2022.07.445.

Singh, B.P., Singh, J., Singh, J., Bhayana, M., Singh, K. and Singh, R. (2022) 'Experimental examination of the machining characteristics of Nimonic 80-A alloy on wire EDM', *Materials Today: Proceedings* [online] https://doi.org/10.1016/j.matpr.2022.08.537.

Sivakumar, S., Khan, M.A. and Muralidharan, B. (2020) 'Studies on surface quality of stainless steel implant material while machining with WEDM process', *International Journal of Machining and Machinability of Materials*, Vol. 22, No. 5, pp.374–385.

Tilekar, S., Das, S.S. and Patowari, P.K. (2014) 'Process parameter optimization of wire EDM on aluminum and MS by using Taguchi method', *Procedia Materials Science*, Vol. 5, pp.2577–2584, https://doi.org/10.1016/j.mspro.2014.07.518.

Uyar, A., Sahin, O., Nalcaci, B. and Kilicli, V. (2022) 'Effect of austempering times on the microstructures and mechanical properties of dual-matrix structure austempered ductile iron (DMS-ADI)', *International Journal of Metalcasting*, Vol. 16, pp.407–418 [online] https://doi.org/10.1007/s40962-021-00617-4.

Vignesh, M. and Ramanujam, R. (2018) 'Response optimisation in wire electrical discharge machining of AISI H11 tool steel using Taguchi-GRA approach', *International Journal of Machining and Machinability of Materials*, Vol. 20, No. 5, pp.474–495.

Wang, C., Liu, R., Li, S., Gu, C., Du, X., Sun, Y. and Tian, J. (2019) 'Effect of austempering temperature on microstructure of ausferrite in austempered ductile iron', *Materials Science and Technology*, Vol. 35, No. 11, pp.1329–1336.

Wang, J., Kunied, M., Sanchez, J.A., Izquierdo, B. and Ayesta, I. (2022) 'Insight on relation between discharge delay time and machining parameters in wire EDM', *Procedia CIRP*, Vol. 113, pp.289–293 [online] https://doi.org/10.1016/j.procir.2022.09.161.

Zhang, Y., Guo, E., Wang, L., Zhao, S., Liu, X., Yi, P., Li, Y., Feng, Y. and Song, M. (2021) 'Insights into effect of first-step austempering temperature on the microstructure and properties of austempered ductile iron', *Materials Research Express*, Vol. 8, No. 8, p.86512.